2017-05-04

The Effects of Dispersants on the Spatiotemporal Distribution of Hydrocarbons: Insights from the Gulf Science Data on the Nature of the Macondo Blowout

Marcia L. Trillo
University of Miami, marciatrillo@gmail.com

UNIVERSITY OF MIAMI

THE EFFECTS OF DISPERSANTS ON THE SPATIO-TEMPORAL DISTRIBUTION OF HYDROCARBONS: INSIGHTS FROM THE GULF SCIENCE DATA ON THE NATURE OF THE MACONDO BLOWOUT

By

Marcia L. Trillo

A THESIS

Submitted to the Faculty

of the University of Miami

in partial fulfillment of the requirements for

the degree of Master of Science

Coral Gables, Florida

May 2017

UNIVERSITY OF MIAMI

A thesis submitted in partial fulfillment of

the requirements for the degree of

Master of Science

THE EFFECTS OF DISPERSANTS ON THE SPATIO-TEMPORAL DISTRIBUTION OF HYDROCARBONS: INSIGHTS FROM THE GULF SCIENCE DATA ON THE NATURE OF THE MACONDO BLOWOUT

Marcia L. Trillo

Approved:

_____ Claire B Paris, Ph.D. Associate Professor Ocean Sciences	_____ M. Josefina Olascoaga, Ph.D. Associate Professor Ocean Sciences
_____ Zachary Aman, Ph.D. Associate Professor School of Mechanical and Chemical Engineering The University of Western Australia	_____ Guillermo Prado, Ph.D. Dean of the Graduate School

TRILLO, MARCIA L. (M.S., Ocean Sciences)
(May 2017)

The Effects of Dispersants on the Spatio-temporal Distribution of Hydrocarbons: Insights from the Gulf Science Data on the Nature of the Macondo Blowout

Abstract of a thesis at the University of Miami.

Thesis supervised by Professor Claire B. Paris.
No. of pages in text. (48)

During the Deepwater Horizon accident in 2010, oil spilled into the Gulf of Mexico and approximately 770,000 gallons of chemical dispersants were injected directly at the Macondo wellhead attempting to keep the oil submerged. Despite conducting thorough research in the past seven years, a detailed empirical analysis as the oil was spewing from the wellhead and after the well capping, has not yet been completely undertaken.

Recently, BP made available a unique dataset ("Gulf Science Data") of oil samples collected from May 2010 to July 2012. In this research, we examine this comprehensive dataset to determine the spatial-temporal distribution of the chemical signature of Macondo oil up to December 2010. Oil samples are classified monthly in two hydrocarbon categories (i.e., C5-C12 and C13+) and the distance from the wellhead is also computed for these classifications in order to better analyze the different hydrocarbon partitioning in the water column. We also analyze the hydrocarbon chemical data depending on the variable dispersant application period to provide an exhaustive sub-sea dispersant injection (SSDI)

analysis. Additionally, the Gulf Science dataset is also used to investigate the role of Earth's rotation on the plume dynamics.

Our spatial data results confirm the presence of the so called "deep-plume" (i.e. a dominant intrusion layer centered around 1,100 m) and show a clear vertical partition of heavier hydrocarbons higher in the water column, which is partly explained by the physical properties of the hydrocarbon chain length. The SSDI robust linear regression analysis reveals no significant differences on the vertical structure of the oil plume with variable dispersant injection, ranging from no dispersant to ca. 22,000 gal/day, thus questioning the effects of SSDI for deep-sea oil spills. Despite inhomogeneous sampling, the comprehensive BP Gulf Science Data sheds some light on understanding the nature of deep blowouts and required responses.

ACKNOWLEDGEMENTS

First and foremost, I want to acknowledge my advisor, Dr. Claire Paris, for all her support throughout this process to complete my Master's degree. I'm very thankful for her guidance, encouragement and financial support during this journey. Being a graduate student and doing scientific research is a challenge, and I could have not made it without her help. Being part of Paris Lab has given me invaluable professional opportunities to grow as a scientist.

I also want to thank those who have helped me complete my thesis, mainly my committee members: M. Josefina Olascoaga and Zachary Aman. I really appreciate their professional expertise and academic guidance throughout this process. Igal Berenshtein has also been extremely helpful with me, providing me with his intellectual knowledge in statistics and improving the methods of my research.

What is life without friends? I've been very lucky to meet wonderful people: Matt, Romain, Camilla, Laura, Mariana, Carlie, Kay, Jaz, but especially Alessandro. He has been a very important person for me in these two years I've lived in Miami. Calling him friend is not even enough, he is like my brother.

I also want to thank Craig, my number-one supporter. Thank you for taking care of me, for helping to find myself when I felt lost, for pushing me forward when I needed it, and for telling me that the sun follows the storm.

I feel blessed for the supportive family that I have. I'm extremely thankful for them, especially my parents. My dad has given me the wisdom I needed in

this journey, and my mum the encourage to move forward. She is the person that misses me the most in the entire planet, so I feel like she also accomplished this masters with me. Special thanks to my grandma Carmen, she is the sweetest and most caring person I've ever met. Last but not least, I want to dedicate this achievement to my grandma Alicia that is guiding me from the sky. She had such a big heart! She is my role model and would have been much happier than I am for what I accomplished.

Finally, I want to acknowledge my funding sources. This work was supported by Fulbright and by the Center for the Integrated Modeling and Analysis of the Gulf Ecosystem (C-IMAGE II) Consortium of the Gulf of Mexico Research Initiative (GoMRI).

TABLE OF CONTENTS

LIST OF FIGURES

LIST OF TABLES

CHAPTER 1: GENERAL INTRODUCTION

On April 20th, 2010, the Deepwater Horizon (DWH) Spill –one of the largest oil blowout disasters in history– took place in the Gulf of Mexico at a depth of 1,522 m. Due to the magnitude of the DWH drilling platform explosion, eleven people died and many others were injured (Graham et al. 2011). The blowout preventer (BOP) was intended to prevent the release of “live oil” (oil and gas mixture) from the wellhead. However, it could not contain the reservoir pressure and led to a severe leakage of 4.1 million barrels of oil (M. McNutt et al. 2011) that spilled into the Gulf of Mexico for 87 days before the wellhead was capped on July 15th, 2010 (Figure 1).

With the attempt to cap the Macondo well MC252, many strategies were carried out. Response efforts included the use of remotely operated underwater vehicles, the utilization of a containment dome, and the installation of the Lower Marine Riser Package (LMRP) after the Riser Cut operation. These actions significantly modified the geometry of the well and consequently altered the oil flow rate, making the evaluation of this deep-sea blowout even more complex. Additionally, a large-scale application of surfactants took place directly at the wellhead with the intention to keep the oil sequestrated in an underwater plume. The DWH event represents a test case for subsea dispersant injection, which had no track record in the field. This novel strategy raised many questions and complicated the assessment of the fate of oil in the water column.

Because the wellhead was at great depth, this unusual oil spill was characterized by high pressure conditions and turbulence. These circumstances may have atomized the oil droplets around the well, naturally contributing with the formation of intrusion layers (R. Camilli et al. 2010, Kessler et al. 2011, Socolofsky et. al 2011, Paris et al. 2012, Valentine et al. 2010, Spier et al. 2013). Given these conditions, not all of the oil surfaced. Gas bubbles and oil droplets were trapped subsurface as they were rising to the water column. An estimation of approximately 2 million barrels of oil remained in the deep sea (M. K. McNutt et al. 2012).

Because of the complexity of this deep ocean oil spill, modeling the fate and transport of the buoyant plume is challenging. There are many parameters that affect the plume dynamics and some of them include: droplet size distribution, gas to oil ratio, dispersant to oil ratio, local pressure, depth and location of the release, background flow dynamics and type of gas and oil spilled. Since the DWH oil spill, important research has been undertaken to simulate this complex oil plume, and numerical models have revealed very important characteristics about this incident (Socolofsky et al. 2015, Lindo-Atichati et al. 2016,Le Hénaff et al. 2012), including an off-axis tilt of the oil plume due to planetary rotation, (Paris et al. 2012, Lindo-Atichati et al. 2016, Fabregat Tomas et al. 2016).

Recently, BP has made available an exhaustive dataset of water samples collected in the Gulf of Mexico during and post the DWH event (1) A comprehensive monthly analysis of the spatial distribution of oil compounds in the water column and at the sea surface has not been fully undertaken yet and is one

of the objectives of this research. Second, this thesis aims to provide a thorough spatial analysis of the hydrocarbon distribution in the Gulf during variable sub-sea dispersant injection (SSDI) periods. And third, we use the Gulf Science Data to potentially confirm the deviation of the oil plume due to Coriolis effect.

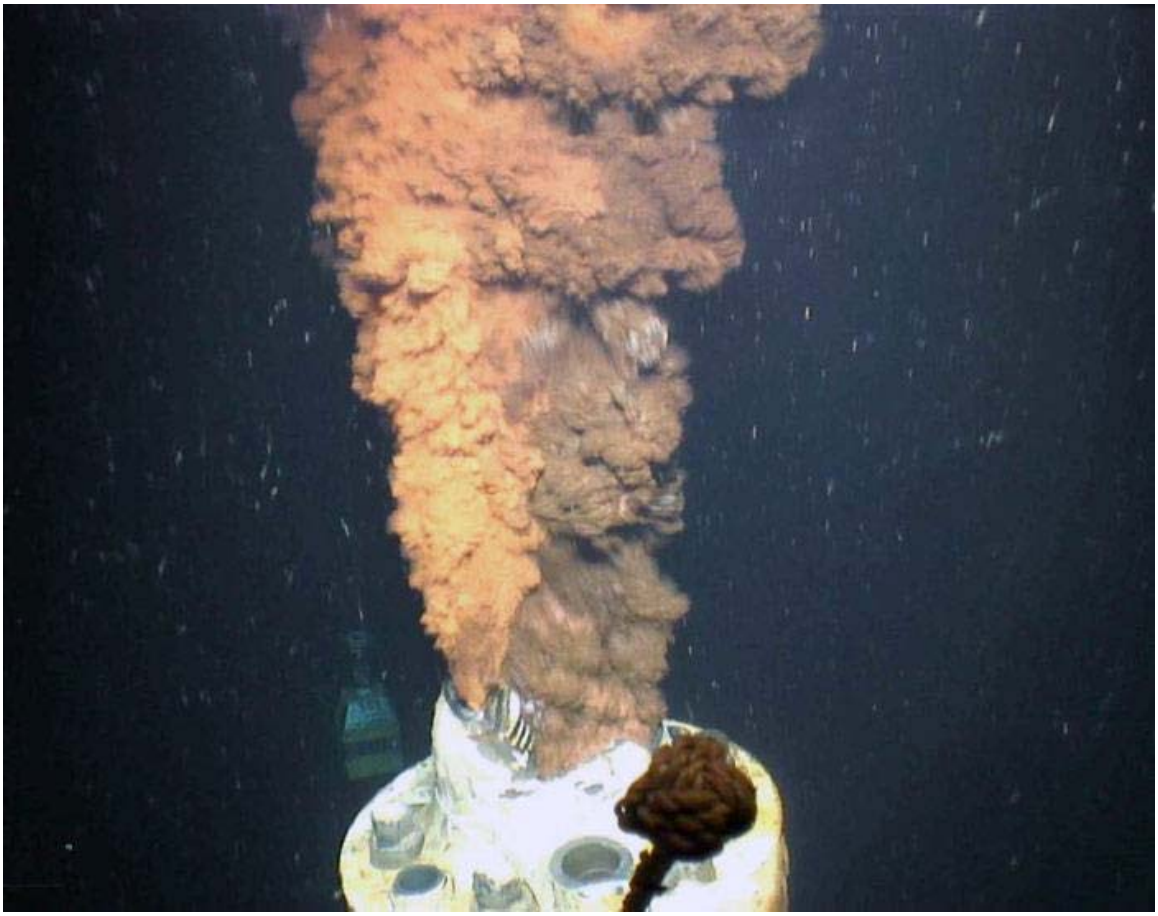

Figure 1. “Live oil” (liquid hydrocarbon saturated with natural gas) flowing into the Gulf of Mexico in 2010 from the broken riser pipe at the Macondo wellhead. *Source: U.S. Geological Survey.*

CHAPTER 2: SPATIO-TEMPORAL DISTRIBUTION OF HYDROCARBONS

Background

Numerous studies have revealed important characteristics about the DWH oil spill. Due to the great depth of the Macondo well, the “live oil” (liquid hydrocarbon saturated with natural gas) behaves very differently than it does in shallower spills. The dynamic physiochemical processes that transport hydrocarbons in the water column depend on the type of oil, the gas-to-oil ratio, the behavior of live oil under high-pressure, and on turbulent and fluctuating flows near the wellhead (Tolman 1949,Greaves et al. 2008). Considering a high flow rate, the buoyant oil plume is naturally dispersed and gets trapped as it rises through the water column as a result of the ambient density stratification, allowing for the formation of intrusion layers (R. Camilli et al. 2010, Kessler et al. 2011, Socolofsky et. al 2011, Paris et al. 2012, Valentine et al. 2010, Spier et al. 2013). A noticeable dominant intrusion, the so-called “deep plume”, was centered at 1,100 m while a second shallower intrusion was identified at about 800 m by (Valentine et al. 2010). The dissolution, biodegradation, and chemical composition of Macondo oil lead to the partition of hydrocarbons as the oil rises in the water column are key processes for deep-sea blowouts (Camilli et al. 2012,Ryerson et al. 2011).

However, a detailed monthly analysis of the spatial distribution of the chemical signature of Macondo oil, as it was flowing from the wellhead and after the well capping, is still missing and is one of the objectives of this study. A comprehensive collection of water samples from more than 67 Response and Natural Resource Damage Assessment (NRDA) studies were recently made available to the scientific community through the BP Gulf Science Data (1). This dataset includes more than 20,000 lab oil results from May 2010 to July 2012, and provides a unique opportunity to examine how the different petroleum hydrocarbons were partitioned in the water column. Here we use a sub sample of the Gulf Science Data water chemistry measurements from May 5 to December 31, 2010 to acquire a mechanistic understanding of the partition and dispersion of petroleum components in the water column during the DWH spill. We provide monthly and detailed spatial analyses of the hydrocarbon distribution both in the water column and at the sea surface to get an insight on the nature of the Macondo blowout.

Data and Methods

The Gulf Science water chemistry data (1) was used for this study. This dataset is a collection of water samples (over 20,000) from more than 67 Response and Natural Resource Management Assessment (NRDA) studies. The water samples were collected in the Gulf of Mexico from May 2010 to July 2012.

The spatial representation of the stations selected for this study is shown in (Figure 2.1). Only water samples further than 1 km offshore were used, because the focus of this study was on evaluating oil in pelagic environments (Gulf of Mexico) rather than in coastal or estuarine areas.

Studies have revealed that, in deep- sea blowouts, the dissolution, biodegradation and chemical composition of crude oil result in the partitioning of hydrocarbons throughout the water column. This partitioning behavior is based on the volatility and aqueous solubility of each hydrocarbon species (Reddy et al. 2012,Ryerson et al. 2011). In order to better understand these processes, the water chemistry laboratory results of Polynuclear Aromatic Hydrocarbons (PAH), alkylated Polynuclear Aromatic Hydrocarbons (aPAH), saturated Hydrocarbons (SHC) and Benzene, Toluene, Ethylbenzene and Xylenes (BTEX) were selected from the Gulf Science dataset and then classified into two categories (Table 2). The designated hydrocarbon groups for this study were: C5-C12 (between five and twelve carbons- intermediate fraction) and C13+ (more than thirteen carbons- heaviest and less volatile fraction).

Most of the data processing was performed using MATLAB R2016b. Following the hydrocarbon classification described before (i.e., C5-C12 and C13+), the water samples that had laboratory replicates were averaged to have a unique concentration result (µg/L) per latitude, longitude, depth and sample date. Although the Deepwater Horizon oil spill began on April 21, 2010, the Gulf Science Data was available from May 5, 2010 and the spatial-temporal representation of hydrocarbons was analyzed monthly from this date until

December 19, 2010. The distance from the wellhead was computed separately for all the water samples selected for the study.

Results and Discussion

Oil droplets rise to the surface depending on their buoyancy relative to the surrounding density stratification. Due to their varying rise rates, they follow different trajectories depending on their size and chemical composition. The lighter compounds (C5-C12) generally rise faster, while the heaviest category (C13+) experiences longer residence times in the water column, on its way towards the surface.

Due to the irregular spatial and temporal distribution of the Gulf Science sampling stations, a substantial heterogeneity of Macondo oil through the water column was observed. This characteristic was present from May to December, 2010 in the two hydrocarbon categories evaluated (Figures 2.2. and 2.3.). The variable oil flow rate during the spill, the subsea dispersant injection at the wellhead, the dissolution, biodegradation and partitioning of hydrocarbon constituents and the ocean dynamic interactions are also important factors that account for the uneven spatial distribution of the oil compounds. A total number of 13,218 of water samples were analyzed for the study. The sampling locations that were positioned less than 100 km from the wellhead were selected for the spatial-temporal representation of hydrocarbons (7,741 for C5-C12 and 7,137 for C13+). Concentrations ranged from 0 to 58,730 µg/L and 0 to 101,768 µg/L for

C5-C12 and C13+, respectively. These highest concentration values were observed in May, during the blowout, and they were located in the >1000m depth range approximately 300 m away from the Macondo well.

As observed in Figure 2.2, from May to July 2010, high concentration values of this hydrocarbon intermediate chain length were radially distributed within approximately 25 km from the wellhead; and were mostly concentrated in the deepest intrusion layer around 1,100 m. In addition, some sampling stations were positioned at the surface, where relatively high hydrocarbon values were found, near the wellhead. In June 2010, the spatial distribution of this category was more dispersed throughout the water column, forming a noticeable rising plume to the surface. After July 2010, the month in which wellhead was capped, most of the concentration values are very low, suggesting the dissipation and dispersion of this intermediate molecular weight hydrocarbon category.

In the case of the category with the longest hydrocarbon chain (Figure 2.3.), elevated values were also present from May to July 2010. They were concentrated around the 1,100 m intrusion layer within a radial 25 km distance from the wellhead, and at the sea surface, at a further distance from the Macondo well (approximately within 75 km). However, especially for June 2010, higher concentration values were mainly observed around the deep plume and also in shallower depths throughout the water column, suggesting the sequestration of oil in shallower intrusion layers. Additionally, compared to the lighter hydrocarbon category, higher concentration values were observed even in the absence of continuous leaking oil after July 2010. These dense oil

constituents experience longer residence times, allowing for the high molecular weight hydrocarbons to disperse more effectively until December, 2010.

Conclusion

The spatial-temporal distribution of oil constituents in the water column depends on each species' aqueous phase solubility and volatility. The lighter category (C5-C12) dissipates earlier from the environment and its chemical signature is not clearly evident after the wellhead capping. However, observations indicate the presence of high concentration values of the heaviest oil compounds even after the wellhead was capped in July 2010. This hydrocarbon category (C13+) contains most of the heavy PAHs, which are highly toxic for the marine environment. Our analysis shows empirical evidence of the deep plume from May to July 2010 centered around 1,100 m. and comprised of oil from both hydrocarbon categories.

C5-C12	cis-Decalin	Dibenzothiophene		
	trans-Decalin	C1-Dibenzothiophenes		
	cis/trans-Decalins	C2-Dibenzothiophenes		
	C1-Decalins	C3-Dibenzothiophenes		
	C2-Decalins	C4-Dibenzothiophenes		
	C3-Decalins	1-Methylnaphthalene		
	C4-Decalins	2,6-Dimethylnaphthalene		
	Benzo(b)thiophene	2-Methylnaphthalene		
	C1-Benzo(b)thiophenes	Carbazole		
	C2-Benzo(b)thiophenes	Benzene		
	C3-Benzo(b)thiophenes	Toluene		
	C4-Benzo(b)thiophenes	Ethylbenzene		
	Naphthalene	o-Xylene		
	C1-Naphthalenes	m-Xylene		
	C2-Naphthalenes	p-Xylene		
	C3-Naphthalenes	m&p-Xylenes		
	C4-Naphthalenes	Xylenes, Total		
	Biphenyl	n-Nonane (C9)		
	Dibenzofuran	n-Decane (C10)		
	Acenaphthylene	n-Undecane (C11)		
	Acenaphthene	n-Dodecane (C12)		
C13	Fluorene	C3-Naphthobenzothiophenes	2-Methylanthracene	n-Eicosane (C20)
	C1-Fluorenes	C4-Naphthobenzothiophenes	2-Methylphenanthrene	n-Heneicosane (C21)
	C2-Fluorenes	Benz(a)anthracene	3-Methylphenanthrene	n-Docosane (C22)
	C3-Fluorenes	Chrysene	4/9-Methylphenanthrene	n-Tricosane (C23)
	Anthracene	C1-Chrysenes	4-Methyldibenzothiophene	n-Tetracosane (C24)
	Phenanthrene	C2-Chrysenes	Chrysene	n-Pentacosane (C25)
	C1-Phenanthrenes/Anthracenes	C3-Chrysenes	Chrysene/Triphenylene	n-Hexacosane (C26)
	C2-Phenanthrenes/Anthracenes	C4-Chrysenes	Benzo(b)fluoranthene	n-Heptacosane (C27)
	C3-Phenanthrenes/Anthracenes	Benzo(b)fluoranthene	Benzo(k)fluoranthene	n-Octacosane (C28)
	C4-Phenanthrenes/Anthracenes	Benzo(k)fluoranthene	Dibenz(a,h)anthracene	n-Nonacosane (C29)
	Retene	Benzo(a)fluoranthene	2,6,10 Trimethyldodecane (1380)	n-Triacontane (C30)
	Benzo(b)fluorene	Benzo(e)pyrene	n-Tetradecane (C14)	n-Hentriacontane (C31)
	Fluoranthene	Benzo(a)pyrene	2,6,10 Trimethyltridecane (1470)	n-Dotriacontane (C32)
	Pyrene	Perylene	n-Pentadecane (C15)	n-Tritriacontane (C33)
	C1-Fluoranthenes/Pyrenes	Indeno(1,2,3-cd)Pyrene	n-Hexadecane (C16)	n-Tetratriacontane (C34)
	C2-Fluoranthenes/Pyrenes	Dibenz(a,h)anthracene	Norpristane (1650)	n-Pentatriacontane (C35)
	C3-Fluoranthenes/Pyrenes	Benzo(g,h,i)perylene	n-Heptadecane (C17)	n-Hexatriacontane (C36)
	C4-Fluoranthenes/Pyrenes	1,6,7-Trimethylnaphthalene	Pristane	n-Heptatriacontane (C37)
	Naphthobenzothiophene	1-Methyldibenzothiophene	n-Octadecane (C18)	n-Octatriacontane (C38)
	C1-Naphthobenzothiophenes	1-Methylphenanthrene	Phytane	n-Nonatriacontane (C39)
	C2-Naphthobenzothiophenes	2/3-Methyldibenzothiophene	n-Nonadecane (C19)	n-Tetracontane (C40)

Table 2. Classification of the Gulf Science water samples considered for the study. The hydrocarbon compounds were classified into two categories based on their carbon chain length (i.e., C5-C12: between five and twelve carbons and C13+: more than thirteen carbons).

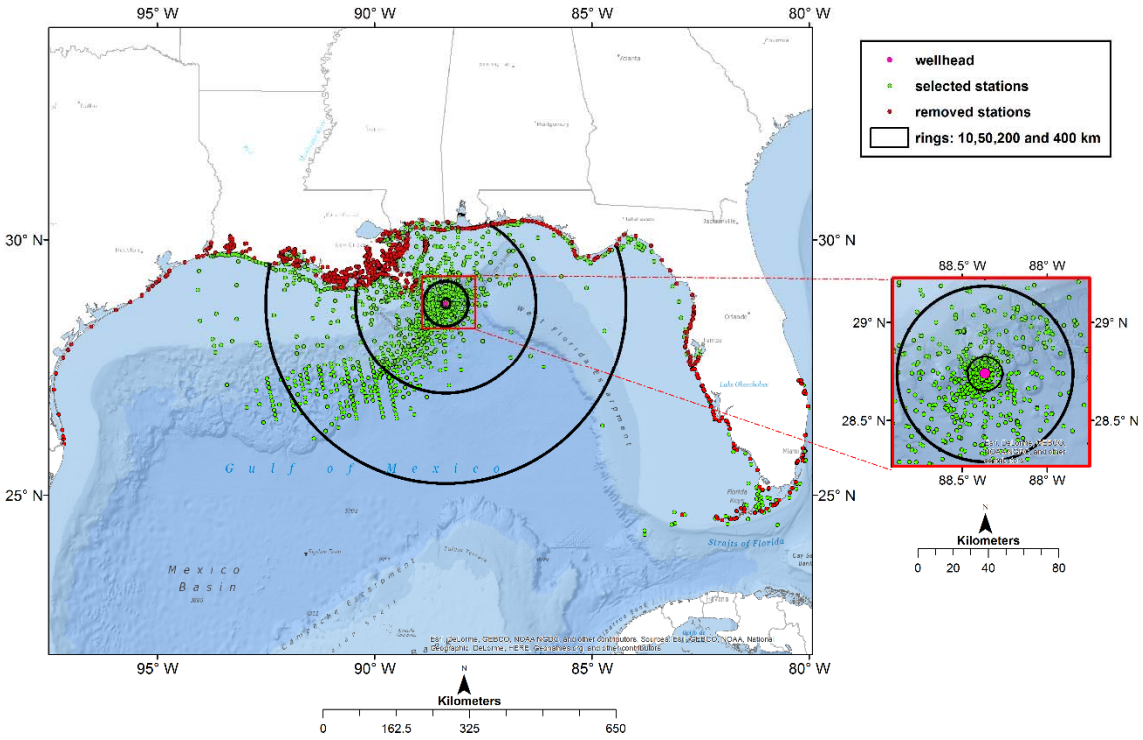

Figure 2.1. Spatial representation of the BP Gulf Science Data stations selected for the study (n =13,218) in the Gulf of Mexico from May, 2010 to December, 2010. The samples that were positioned less than 1 km offshore (n = 2,127) were removed from the analysis. The black rings around the wellhead location were used for the sub-sea dispersant injection (SSDI) analysis in CHAPTER 3.

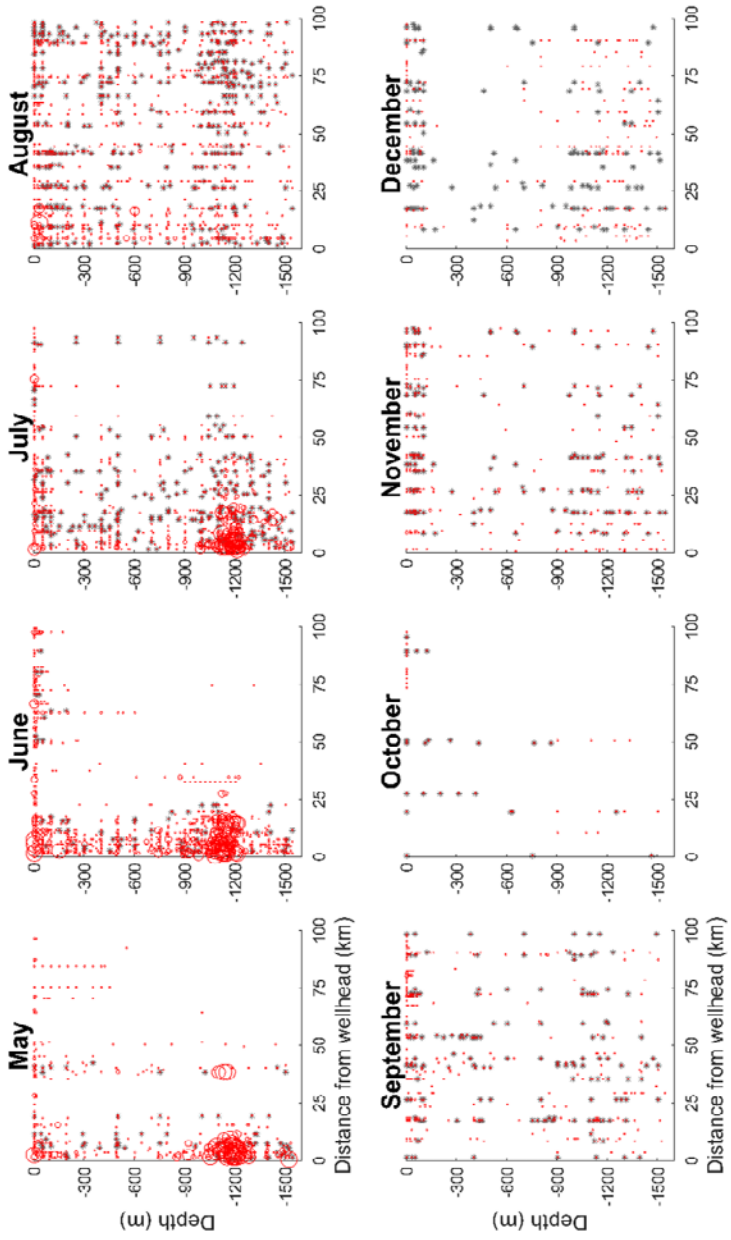

Figure 2.2. Monthly maximum oil concentrations of C5-C12 water samples from May 2010 to December 2010. Data was organized into a grid of 10 m depth by 1 km bins. Grey asterisks represent samples with zero concentration (0 µg/L).

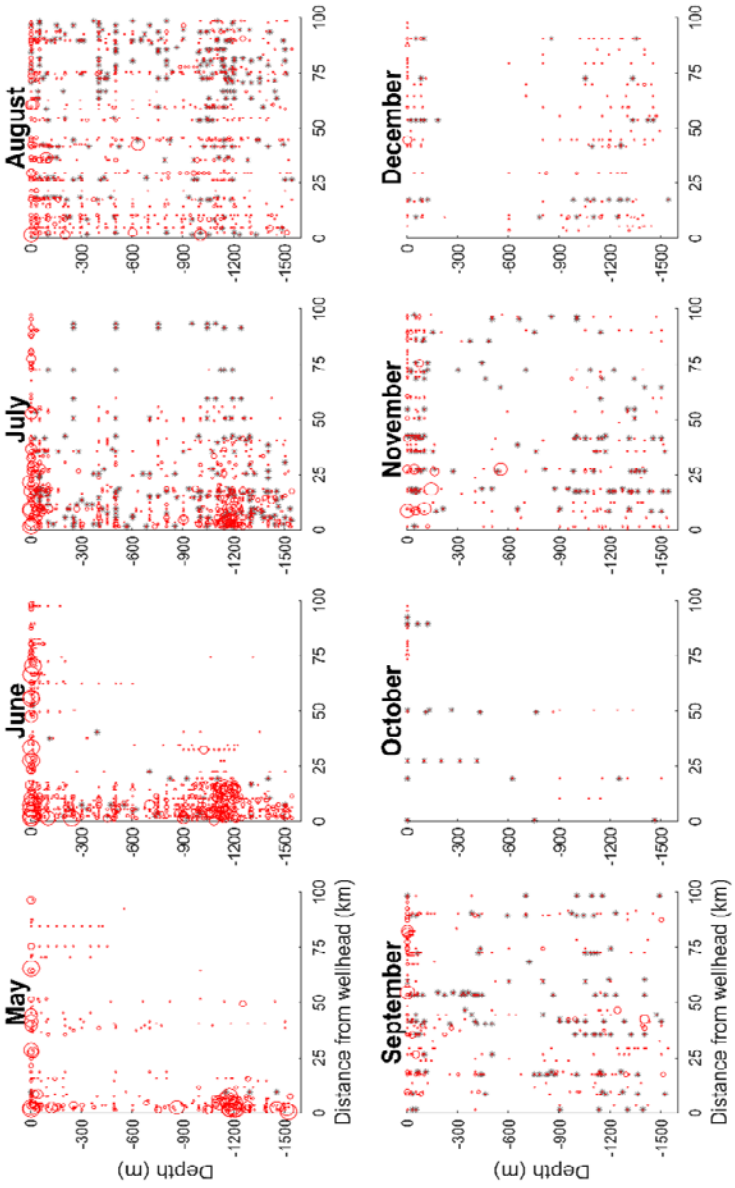

Figure 2.3. Monthly maximum oil concentrations of C13+ water samples from May 2010 to December 2010. Data was organized into a grid of 10 m depth by 1 km bins. Grey asterisks represent samples with zero concentration (0 µg/L).

CHAPTER 3: SUB- SEA DISPERSANT INJECTION (SSDI) ANALYSIS

Background

An unprecedented amount of chemical dispersants, namely Corexit 9500 produced by “Nalco-Champion, an Ecolab company” (2) was injected directly at the wellhead as a first response to prevent the oil from rising to the surface by enhancing the formation of micro droplets (Wilson et al. 2016). In theory, smaller droplets should have been trapped in the subsea plume, together with those generated by high flow rate and pressure drop (Paris et al. 2012, Aman et al. 2015), resulting in longer residence times of dispersed Polynuclear Aromatic Hydrocarbons (PAHs) and other toxic petroleum components in the water column (Diercks et al. 2010,Wade et al. 2013). Additionally, the dispersed oil should have been surfacing slower in thinner sheens downstream from the spill site (Socolofsky et al. 2015), enhancing response efforts. Yet, thus far, little is known about the effects and consequences of sub-sea dispersant injection (SSDI) during deep-sea blowouts. Indeed, during the DWH accident, oil kept rising to the ocean surface despite SSDI, which called to question the effectiveness of this new procedure and complicated the assessment of the oil transport and fate. In this study, we examine the Gulf Science dataset in relation to variable dispersant injection volumes at the wellhead, which allows for further considerations of the effects of SSDI during the Macondo blowout.

Data and Methods

The Gulf Science subsurface and surface dispersant application records (3,4), and the Gulf Science water chemistry data (1) were used for this study. Additionally, the amount of oil discharged from the Macondo well into the Gulf of Mexico (Lindo-Atichati et al. 2016) was also taken into account in the analysis.

Since the SSDI is supposed to disperse the oil into smaller droplets to reduce the amount of oil reaching the ocean surface, the two hydrocarbon categories (i.e., C5-C12 and C13+) of the Gulf Science water chemistry dataset were added together to better account for most of the hydrocarbon compounds that are found in the chemical composition of Macondo oil. Using ArcMap 10.5, the individual distances of the water samples from the wellhead were computed (Geographic Coordinate System: WGS 1984, Projected Coordinate System: World Behrmann), and rings around the Macondo well were created (Figure 2.1.). The depth ranges to examine the oil concentration throughout the water column were selected based on the location of the intrusion layers documented in the Deepwater Horizon (DWH) event (i.e., 0-20m, 20-400m, 400-1000m and >1000m) (R. Camilli et al. 2010, Kessler et al. 2011, Socolofsky et. al 2011, Paris et al. 2012, Valentine et al. 2010, Spier et al. 2013). The dominant intrusion layer (i.e., ‘deep plume’) plays a crucial role in determining the spatial distribution of the hydrocarbons in the water column. It is located around 1,100 m and was well captured in the depth range of >1000 m that was created around the wellhead location.

In order to examine whether the SSDI had an effect on the vertical structure of the oil, we first computed the ratio between the mean oil concentration of the three upper depth ranges (i.e., 0-20 m, 20-400 m and 400-1000 m) and the mean oil concentration of the bottom depth range (i.e., >= 1000 m). For the analysis, we omitted concentration values equal to zero since the hydrophobic nature of the oil results in high patchiness, and the zero concentration between these patches do not realistically represent the spatial plum structure. Moreover, the oil concentration measurement is highly sensitive ($<10^{-5}$ µg/L). We used the water samples that were taken at the same location (<~150 m) on the same day and selected the stations that had water samples for at least the deepest and shallower depth ranges. As there were differences of orders of magnitude in the concentration values, a logarithmic transformation was applied to the oil concentration measurements. Due to the logarithmic transformation, the ratio was computed as the subtraction of log (concentration). Therefore, positive vertical concentration ratio represents higher oil concentration at the three upper depth ranges compared to the deep layer, and a low negative vertical concentration ratio represents a high oil concentration trapped at depth in the deep plume. With the understanding that many factors may affect the vertical structure of the plume, we hypothesized that had the deep dispersant a strong effect on the plume's vertical structure, then the variation in the amount of application would have been reflected in the vertical structure parameter.

The following explanatory variables that could explain the variance of the vertical ratio were: volume of Sub- Sea Dispersant Injection (SSDI) [gal.], volume

of surface dispersant application [gal.], distance from the wellhead [km], flow rate [bbls/day] and time from blowout [days]. The SSDI was daily analyzed with the assumption that Corexit 9500A would reach equilibrium adsorption to the water-oil interface on the timescale of seconds, as a characteristic property of ionic surfactants.

Using R and R Studio, we first applied a multiple linear regression analysis, which revealed the presence of residual outliers- therefore a robust linear regression was applied to reduce the effect of outliers on the model. Briefly, this method is an alternative to the ordinary linear least of squares regression that moderates the influence of outlying cases to provide a more realistic fit to the data. This analysis weights the residuals according to the inverse of their variance instead of giving equal weights to all of the residuals. Regression assumption of multi-collinearity, and autocorrelation test were performed using R and R Studio (5).

Results and Discussion

A total amount of 771,272 gallons of subsea Corexit 9500 (2) were directly injected at the wellhead from April 20 to July 15, 2010 (Figure 3.1.). The dispersant application peaks were reported from June 3 to June 5, 2010, accounting for 58, 714 gallons.

Figures 3.2. and 3.3. show the relationship between the volume of SSDI and the oil concentration with time (from the day of the blowout to the day of the

wellhead capping) in the depth range of more than 1000 m. Theoretically, an increase in oil concentration should be expected when increasing SSDI, because a larger number of small oil droplets should be sequestrated in the dominant intrusion layer as they rise through the water column, together with those generated by natural conditions. However, no evident trend is observed when analyzing the primary data. Additionally, in Figure 3.2. a very high mean concentration value is observed 15 days after the blowout (May 5) in the absence of Corexit 9500. This may reveal the presence of the deep plume, which is naturally generated by the high oil flow rate and high pressure conditions around the wellhead.

Figures 3.4., 3.5 and 3.6. show the nature of the relationship between the volume of SSDI and the oil concentration with time (from the day of the blowout to the day of the wellhead capping) in the surface layer (0-20 m). Dispersants should have maintained a safe and clean response site by preventing the oil from coming to the sea surface. However, with SSDI, high mean concentration values were found locally (near the response site) with no apparent effect of the SSDI.

As shown in the raw data, and for all cases, there is no evident correlation between the volume of SSDI and the oil concentration with time during the Macondo blowout. This coincides with the statistical results of the robust linear regression analysis shown in Table 3.1. The analysis suggests the SSDI did not have a significant effect on the vertical structure of the oil plume ($t = -0.0252$, slope= $9.73*10^{-6}$, $p>0.05$), while controlling for other important factors such as

surface dispersant application, days from the blowout, flow rate, and distance from the wellhead.

To better understand the potential effect of the SSDI on the oil concentration, it is crucial to control the presence of other predictors or explanatory variables that are in the statistical model (i.e., surface dispersant application [gal], time from blowout [days], distance from the wellhead [km] and flow rate [bbls/day]). Figure 3.7. shows the 'added variable' plot of the response variable (vertical concentration ratio) versus the explanatory variable (SSDI) and it accounts for the effect of all the other explanatory variables included in the robust linear regression model. If the SSDI had the desired effect, then we would expect a significant negative correlation, indicating more oil concentration in the deep plume with increasing SSDI. One caveat to this explanation is whether the dispersant was applied above its critical micelle concentration (CMC) in the deep sea; there is insufficient laboratory data to inform whether this may have been the case, whereby an increase in dispersant concentration above CMC would be unlikely to increase surfactant adsorption to the water-oil interface. The data indicate that, no trend between SSDI volume and oil concentration is evident in Figure 3.7. Although a subtle positive correlation is observed (which means that there is more oil in the three upper depth ranges than in the deep plume, with increasing SSDI), the slope of the trendline is close to zero ($y= 9.7*10^{-6}x + 1.4*10^{-17}$). In theory, with this deep injection, there should have been an increase in the hydrocarbon concentration values at depth because the majority of oil micro-droplets generated by the surfactant should have been trapped in the subsea plume located around 1,100m,

together with those generated by natural conditions. However, these results suggest that this operation did not succeed in keeping the oil submerged.

During the blowout, there were natural processes occurring at depth that were possibly leading to the formation of the dominant intrusion layer. From May 8 to May 15 2010, there was a drop of pressure in the blowout preventer (BOP) and an increase in the oil flow rate (Griffiths 2012). Additionally, from June 1 to June 5 2010, the Riser Cut operation took place on top of the BOP, following with the installation of the Lower Marine Riser Package (LMRP) cap. These operations left a cut pipe and also increased the flow rate to approximately 3%. These conditions may have been sufficient enough to increase turbulence and energy of mixing around the wellhead, naturally leading to the formation of the deep plume. However, these dates coincide with low and intermediate SSDI periods (Fig 3.1), respectively. These response efforts complicated the evaluation of the effect of surfactants for deep- sea blowouts, because the deep plume may have already been formed by natural conditions prior to SSDI.

Robust linear regression results also indicate that the time from the blowout ($t= 4.3514$, $slope= 2.1*10^{-2}$, $p= 3.18*10^{-5}$) and the flow rate ($t= 2.1797$, $slope= 1.17*10^{-4}$, $p= 0.03129$) had a positive and significant effect on the oil vertical structure. This may be explained by the fact that the flow rate slightly decreased with time, thus leading to larger oil droplets rising to the sea surface and increasing the value of the oil vertical ratio.

A second intrusion was identified at about 800 m by (Valentine et al. 2010). In order to test the effect of the SSDI on this shallower intrusion layer, a robust

linear regression model was also performed. The response or dependent variable was logarithmically transformed and defined as the ratio between the mean oil concentration of the two upper depth ranges (i.e., 0-20 m and 20-400 m) and the mean oil concentration of the depth range in which the shallower intrusion layer was revealed (i.e., 400-1000 m). Results (Table 3.2. and Figure 3.8.) also show no strong significant effect of the SSDI (slope=$1.60*10^{-5}$, t=0.7811, p=0.4586) on the vertical concentration ratio (response variable).

Conclusion

Statistical results suggest that there was no strong effect of the SSDI on the vertical oil distribution during the Macondo blowout. High energy of mixing and turbulent conditions at the wellhead generated natural dispersion (Aman et al. 2015). In addition, the oil kept rising to the sea surface and near the response site even with high SSDI, which indicates that other processes not accounted for in the response strategy -such as gas saturation effects were taking place and were altering the droplet size distribution as the oil was rising through the water column. These conclusions were previously supported both by computer modeling and high-pressure experiments (Paris et al. 2012,Aman et al. 2015). The lack of apparent effect of the SSDI does not necessarily mean, that it did not have an effect, but rather indicate that other natural processes (e.g. biodegradation and evaporation) probably had a much stronger effect, masking the effect of the SSDI. Given that natural processes may completely dictate the dynamics of the oil plume

and that Corexit 9500A leads to adverse toxic effects, SSDI should not be a routine response for deep-sea blowouts. Its routine application should be revisited following our findings.

	p- value	F-statistic	t- value	std. error	slope values	y-intercepts
(Intercept)			-2.512	3.1628	-7.9447	
SSDI [gal]	**0.9801**	**0.0006259**	**-0.0252**	**0**	**$9.73*10^{-6}$**	**$1.43*10^{-17}$**
Surface dispersant application [gal]	0.3277	0.96706	-0.9834	0	$-2.48*10^{-5}$	$-2.83*10^{-17}$
Time from blowout [days]	$3.18*10^{-5}$	18.945	4.3514	0.0049	$2.10*10^{-2}$	$-3.13*10^{-18}$
Distance from the wellhead [km]	0.8633	0.029793	0.172	0.0214	$1.78*10^{-3}$	$1.87*10^{-17}$
Flow rate [bbls/day]	0.03129	4.7667	2.1797	0.0001	$1.17*10^{-4}$	$9.69*10^{-18}$
SSDI: Surface dispersant application interaction [gal]			0.6763	0	$1.00*10^{-9}$	$5.00*10^{-17}$

Table 3.1. Robust linear regression model between the explanatory variables and the response variable, i.e., vertical oil concentration ratio: logarithmic transformation of the mean of the three upper layers minus the mean of the bottom depth range where the deep plume was documented. We used oil concentration data within 10 km of the wellhead. The residual standard error of the model is 0.558 on 103 degrees of freedom, n=110.

	p-value	F-statistic	t- value	std. error	slope values	y-intercepts
(Intercept)			-0.4328	3.6503	-1.58	
SSDI [gal]	**0.4586**	**0.56831**	**0.7811**	**0**	**$1.60*10^{-5}$**	**$-2.03*10^{-17}$**
Surface dispersant application [gal]	0.6353	0.23106	0.4653	0	$1.24*10^{-5}$	$5.16*10^{-18}$
Time from blowout [days]	0.6245	0.24616	0.5027	0.0067	$1.20*10^{-2}$	$-1.01*10^{-17}$
Distance from the wellhead [km]	0.9467	0.0045692	0.0656	0.0265	$1.33*10^{-2}$	$-1.61*10^{-18}$
Flow rate [bbls/day]	0.7368	0.11576	0.3433	0.0001	$5.80*10^{-5}$	$-1.01*10^{-17}$
SSDI: Surface dispersant application interaction [gal]			-0.2653	0	$-5.00*10^{-10}$	$-2.00*10^{-16}$

Table 3.2. Robust linear regression model between the explanatory variables and the response variable, i.e., vertical oil concentration ratio: logarithmic transformation of the mean of the two upper layers minus the mean of the 400-1000 m depth range where the plume centered around 800 m. was documented. We used oil concentration data within 10 km of the wellhead. The residual standard error of the model is 0.1505 on 23 degrees of freedom, n=30.

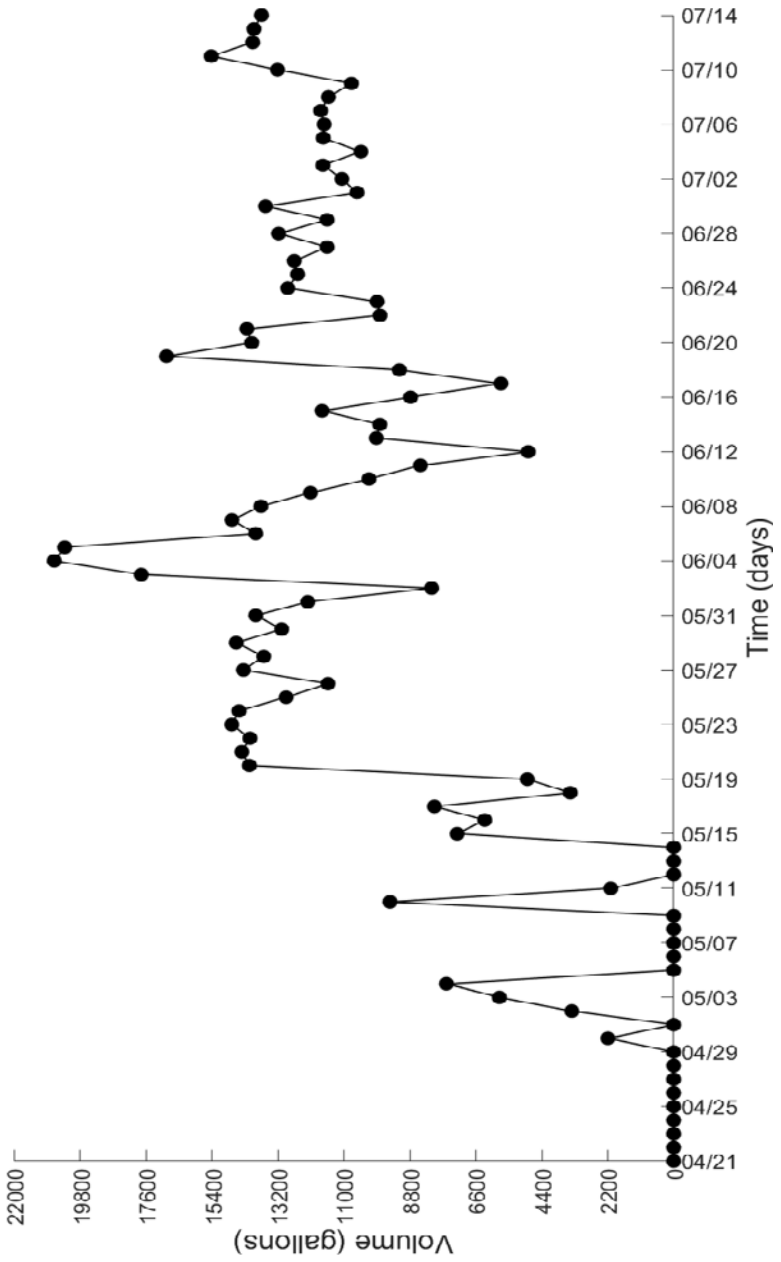

Figure 3.1. Time series of sub-sea dispersant injection (SSDI) time series from April 21, 2010 (1st day of the blowout) to July 15, 2010 (corresponding to the capping of the Macondo wellhead). The SSDI application was not uniform throughout the time series. There were periods with no SSDI and periods with low, intermediate and high SSDI.

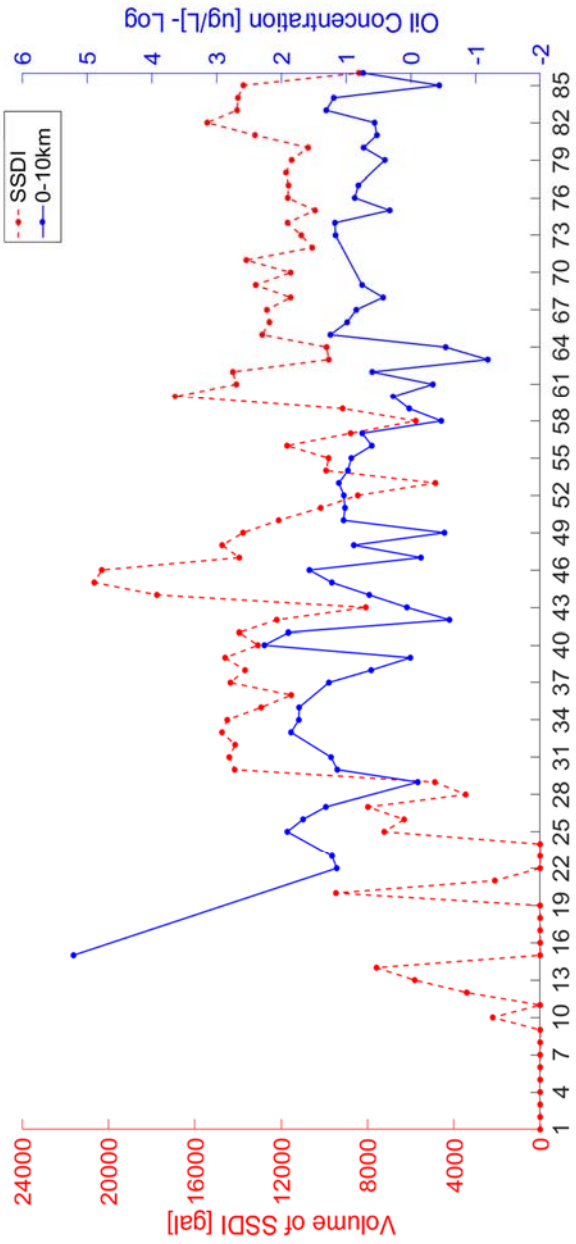

Figure 3.2. Daily Sub-Sea Dispersant Injection (SSDI) in relation to oil concentration below 1000 m. The data was computed within a radius of 10 km from the Macondo wellhead since SSDI occurred directly at the wellhead into the flow of oil and gas. There is not positive correlation between SSDI and oil concentration at depth as expected from the effectiveness of the procedure.

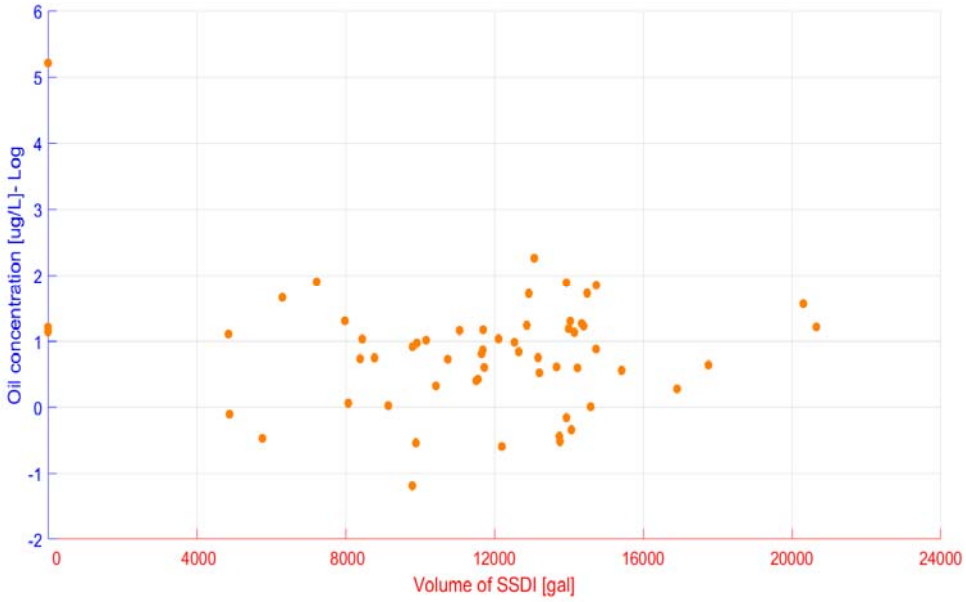

Figure 3.3. Relationship between oil concentration below 1000 m and volume of SSDI. The data was computed within a radius of 10 km from Macondo, since its application occurred directly at the wellhead into the flow of oil and gas. There is no significant correlation between the oil concentration and the volume of SSDI. In addition, a high mean concentration value is observed with no SSDI, which indicates the presence of the “deep plume” generated by natural dispersed conditions.

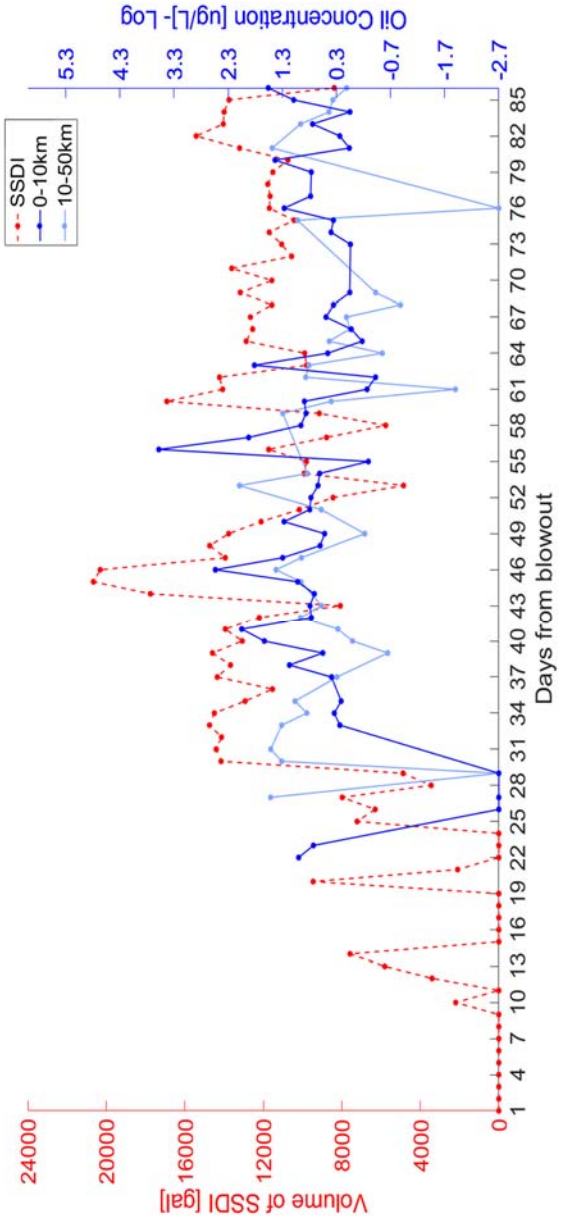

Figure 3.4. Daily Sub-Sea Dispersant Injection (SSDI) in relation to oil concentration for the sea surface (0-20 m). The data was computed separately for 0 to 10 km and from 10 to 50 km from the wellhead. If the SSDI had the desired effect, oil should not rise to the surface. However, there is no correlation between the SSDI and oil concentration at the sea surface.

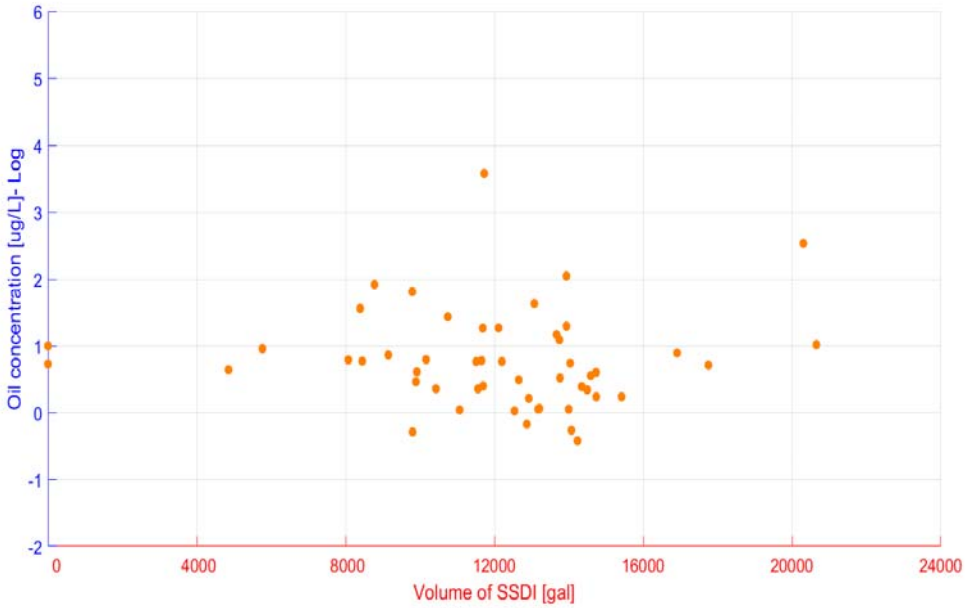

Figure 3.5. Relationship between oil concentration and volume of SSDI at the sea surface (0-20 m). The data was computed within a radius of 10 km from Macondo. If the SSDI had the desired effect, oil should not rise to the surface. However, oil is rising to the surface, and close to the response site when sub-sea dispersant is applied. There is no significant correlation between the SSDI and oil concentration.

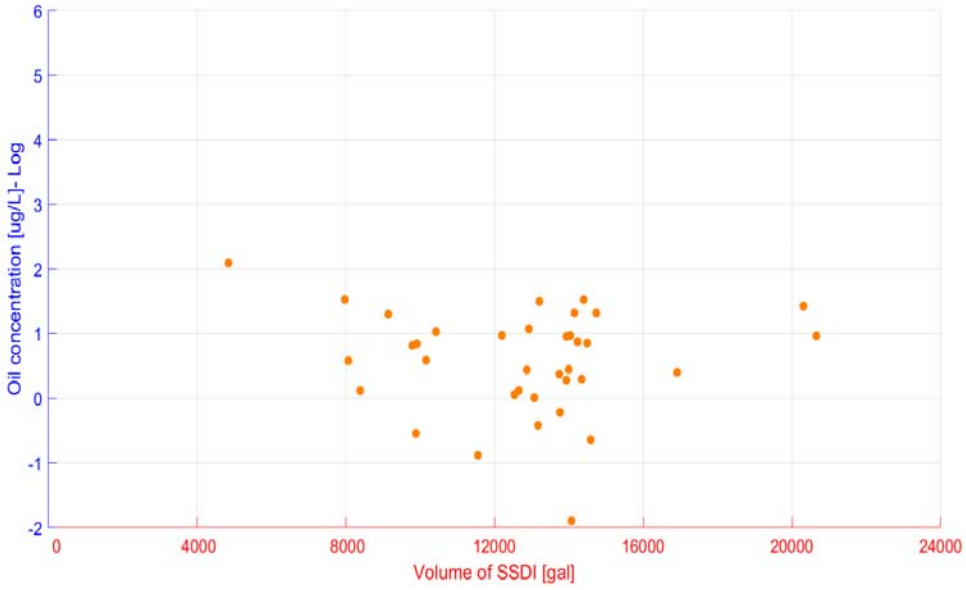

Figure 3.6. Relationship between oil concentration and volume of SSDI at the sea surface (0-20 m). The data was computed between 10 and 50 km from the Macondo well. If the SSDI had the desired effect, oil should not rise to the surface. However, oil is rising to the surface, and also further from the wellhead when sub- sea dispersant is applied. There is no significant correlation between the SSDI and oil concentration.

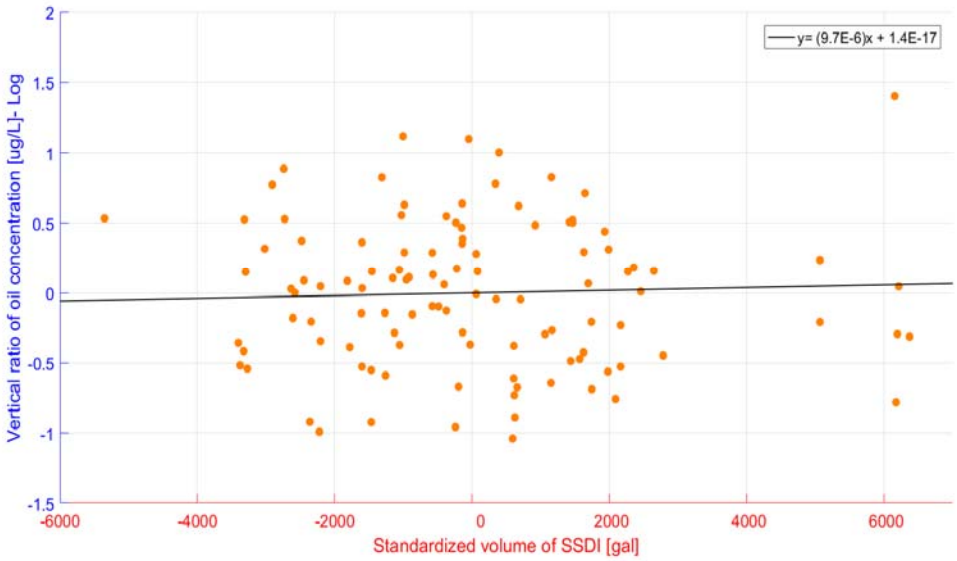

Figure 3.7. Robust linear regression model: 'added variable' plot of the vertical ratio of oil concentration [ug/L] (mean concentration of the three upper depth ranges over the depth range where the deep intrusion was identified) versus the standardized volume of SSDI [gal]. The data is computed within a 10 km radius from the Macondo wellhead. There is no significant correlation between the response variable and the independent variable.

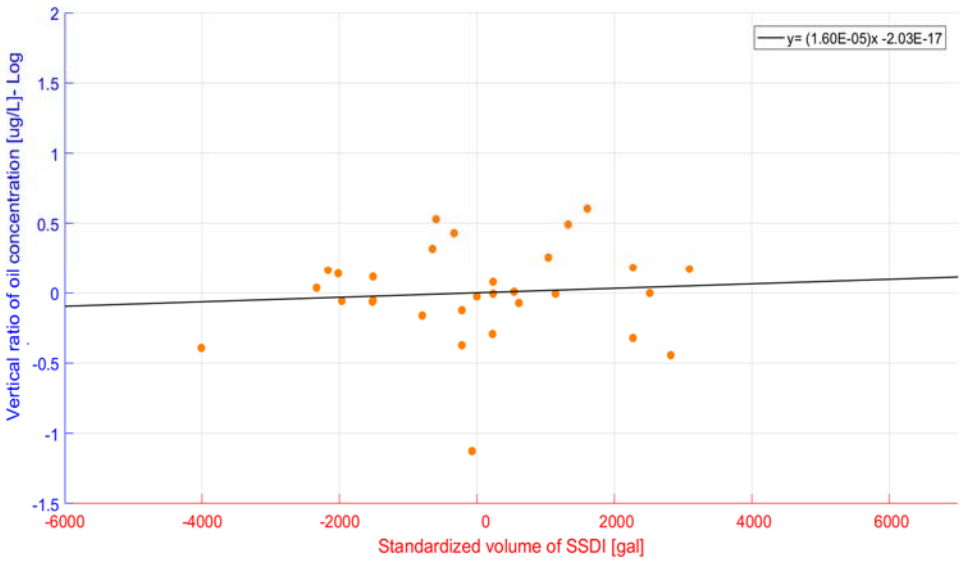

Figure 3.8. Robust linear regression model: 'added variable' plot of the vertical ratio of oil concentration [ug/L] (mean concentration of the two upper depth ranges over the 400-1000 m where the shallower intrusion was identified) versus the standardized volume of SSDI [gal]. The data is computed within a 10 km radius from the Macondo wellhead. There is no significant correlation between the response variable and the independent variable.

CHAPTER 4: OFF- AXIS DEVIATION OF THE OIL PLUME

Background

Coriolis force is likely to play a very important role in the plume dynamics since oil spilled for 87 days and the plume remained in the water column even after the wellhead was capped on July 15th, 2010 (Paris et al. 2012, Lindo-Atichati et al. 2016, Fabregat Tomas et al. 2016). An anticyclonic rotation, suggested to be driven by the Coriolis and pressure gradient forces, was revealed by a coupled hydrodynamic and far-field model in (Paris et al. 2012). This clockwise feature was also very well captured for constant and variable flow rate experiments and for different times during the year 2010 (Lindo-Atichati et al. 2016). This planetary-induced turn may affect the circulation around the oil plume by creating mixing in the water column. The earth's rotation role in the plume dynamics has not been fully addressed yet, and in this study the Gulf Science Data is also analyzed to determine the potential tilt direction of the oil plume caused by Coriolis force (Fabregat Tomas et al. 2016). In our research, we select the oil samples collected in May 2010 and represent them with respect to the distance from the wellhead, in order to determine their location and potentially confirm the Coriolis effect.

Data and Methods

The DWH oil spill started on April 21, 2010 and the off-axis tilt of the oil plume was very well captured at the sea surface by a satellite image on April 29, 2010 approximately centered at 20 km from the wellhead. (Figure 4.1). For the analysis, we used this satellite image in order to estimate the distance of the oil plume deviation and selected the Gulf Science water samples for May, 2010. We combined both hydrocarbon categories (i.e., C5-C12 and C13+) by adding the oil concentration values together. It is likely that from June, 2010 other ocean dynamic factors could affect the behavior of the plume, and this is the reason why we selected the month after the DWH event started to better account for the Coriolis effect. A persistent anticyclonic precession of the plume axis for deep-sea blowouts was revealed in (Fabregat Tomas et al. 2016). The Rossby number (Ro) is defined as stratification over rotation, which is characterized by the buoyancy frequency over the rotation frequency. A representative Ro for the Deepwater Horizon oil spill was estimated as 10. Given these characteristics, and when comparing with non-rotating cases, the precession angle of this plume axis deflection with respect to the vertical z- axis in the near-source region was found to be approximately 66**°.** Assuming this linearity, to determine the deviation angle (Figure 4.2.), we assumed that the tilt of the oil plume approximately coincides with the hypotenuse of a right triangle, being its legs 1,522 m (depth of the wellhead) and 20 km (distance of the oil slick from the wellhead, Figure 4.1). Given that the horizontal length scale of the ocean is much

larger than the vertical length scale, the resulting angle is 85° 35' 60", which is very close to 90° 0' 0.

Results and Discussion

In Figure 4.3., high maximum concentration values are observed within a radial distance of approximately 8 km from the wellhead, and they are laterally distributed around the dominant intrusion layer centered at 1,100 m. Elevated oil concentration is also observed at the sea surface within approximately 4 km from the wellhead. Ideally, if the oil plume was tilted, the spatial distribution of the maximum oil concentration values should be different. We would expect most of them to be located in the area determined by the two dashed lines and the sea surface (between 15 and 25 km). We considered this variation range of 10 km at the sea surface because complex physical processes are expected, such as turbulence, advection and mixing. As depth increases and the distance from the wellhead decreases, the variation range decreases too and the analysis is more accurate.

Conclusion

We do not observe an off-axis tilt of the oil plume with the empirical data we used for the study. There is clear evidence of the dominant intrusion layer centered at 1,100 m, and high maximum oil concentration values are also

observed at the sea surface, close to the wellhead (within approximately 8 km) and not between 15 and 25 km (the ideal range if the oil plume was tilted). Because an off- axis tilt was not observed with the water samples of May 2010, the water samples from May 2010 to July 2010 (the period during the DWH oil spill until the wellhead capping) were also computed against the distance from the wellhead (Figure 4.4.). There was no evidence of the oil plume tilt within these 3 months either. It could be possible that the oil plume followed other type of curve, such as a nonlinear shape on its way towards the surface. There are still variables that must be considered to better isolate the planetary rotation effect, such as the surface layer and the dominant deep intrusion layer. The sea surface is a highly complex layer affected by multiple ocean and atmospheric processes such as turbulence (driven primarily by the surface wind stress and convective buoyancy flux), horizontal advection and surface heating. Although our study was based on the satellite image of April 29, 2010 (Figure 4.1.), it could have been possible that the oil slick was closer or further away from the wellhead (due to the complex aforementioned processes) before April 29, changing the oil plume deviation distance at the ocean surface. This could affect the off-axis angle to less or greater than 85° 35' 60", which could explain the discrepancy with the precession angle of 66° revealed by (Fabregat Tomas et al. 2016). Furthermore, rotating plumes are distinguished by a decrease in vertical buoyancy and momentum fluxes, leading to lower and thicker neutrally buoyant intrusion layers (Fabregat Tomas et al. 2016). Our results confirm the presence of the dominant intrusion layer revealed in the Deepwater Horizon event (R.

Camilli et al. 2010, Kessler et al. 2011, Socolofsky et. al 2011, Paris et al. 2012, Valentine et al. 2010, Spier et al. 2013). The effect of planetary rotation in the near-source region could be masked by the existence of this deep-plume, where high oil concentration values are clustered laterally around 1,100 m (Figures 4.3. and 4.4.). Additionally, the Gulf Science stations were characterized by highly irregular spatial-temporal distribution and further tracking of the hydrocarbons' mass flux is necessary to understand their fate in the water column.

Figure 4.1. Off-axis tilt of the oil plume at the sea surface on April 29, 2010. The center of the surface expression of the oil jet plume is at approximately 20 km from the wellhead (red dot). Source: National Aeronautics and Space Administration (NASA).

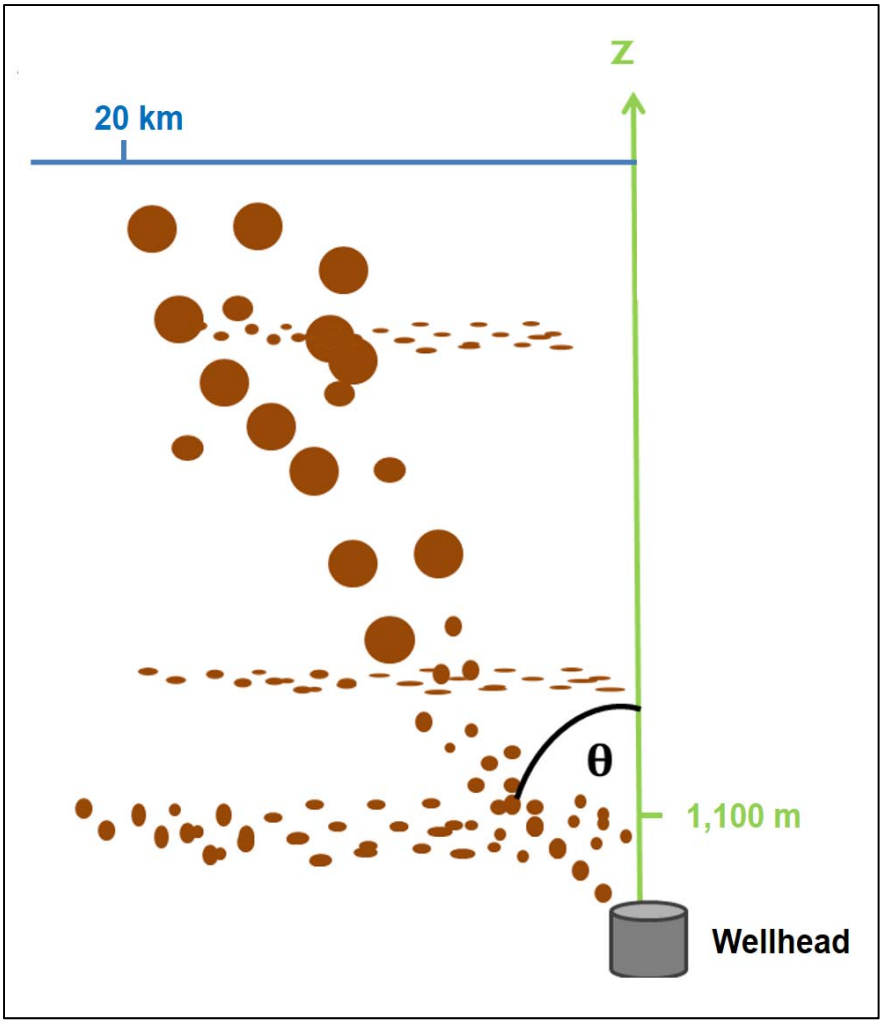

Figure 4.2. Schematic representation of the off- axis deviation from the oil plume from the vertical-axis. The smallest oil micro-droplets form the deep plume (dominant intrusion centered at 1,100 m), while larger droplets leave the jet to form shallower intrusions. The angle Θ 85.6 ° is estimated based on the depth of the wellhead (1,522 m) and the distance (20 km) of the oil slick at the sea surface from the wellhead location during April 29, 2010 (Fig. 4.1.). In theory, high oil concentration values close to the hypotenuse of the right triangle would confirm the effect of planetary rotation. Note: the figure is not to scale.

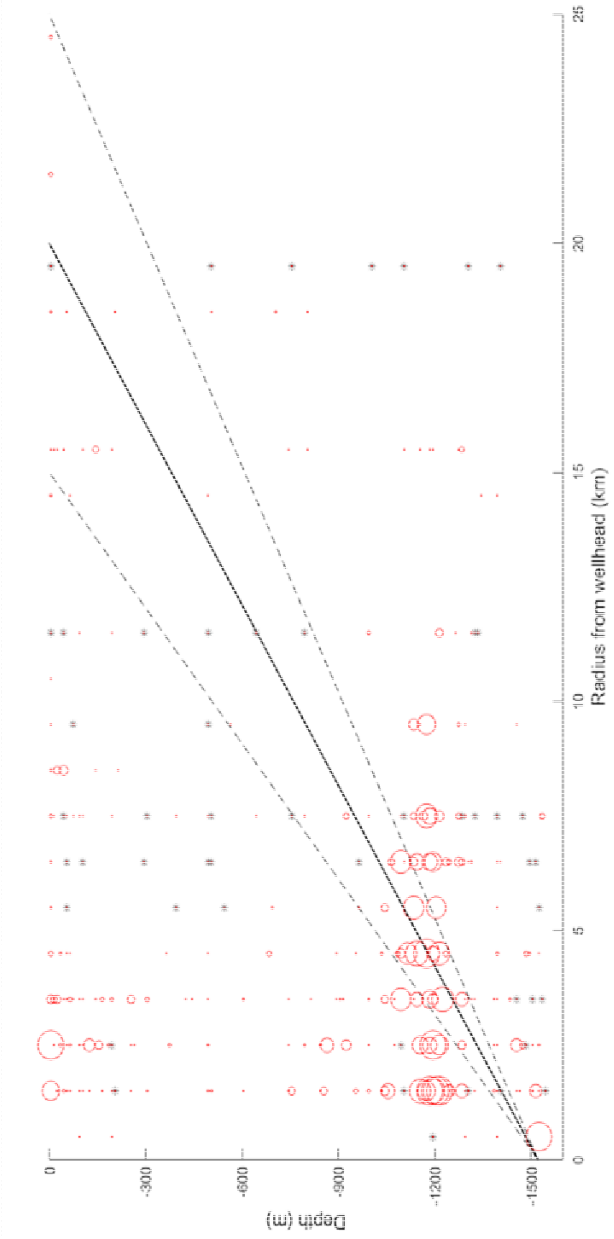

Figure 4.3. Maximum oil concentrations of all BP Gulf Science Data water samples collected during May, 2010. The oil concentration is computed for both hydrocarbon categories C5-C12 and C13+. Data is organized into a grid of 10 m (depth) by 1km (radial distance from wellhead) bin. The size of the red circles is proportional to the oil concentration values. Grey asterisks represent samples with zero concentration (0 µg/L). The red solid line indicates the hypotenuse of the ideal right angle, and the dashed lines represent hypotenuses with a distance from the wellhead from 15 to 25 km at the sea surface, to account for spatial variation in the tilt of the jet plume.

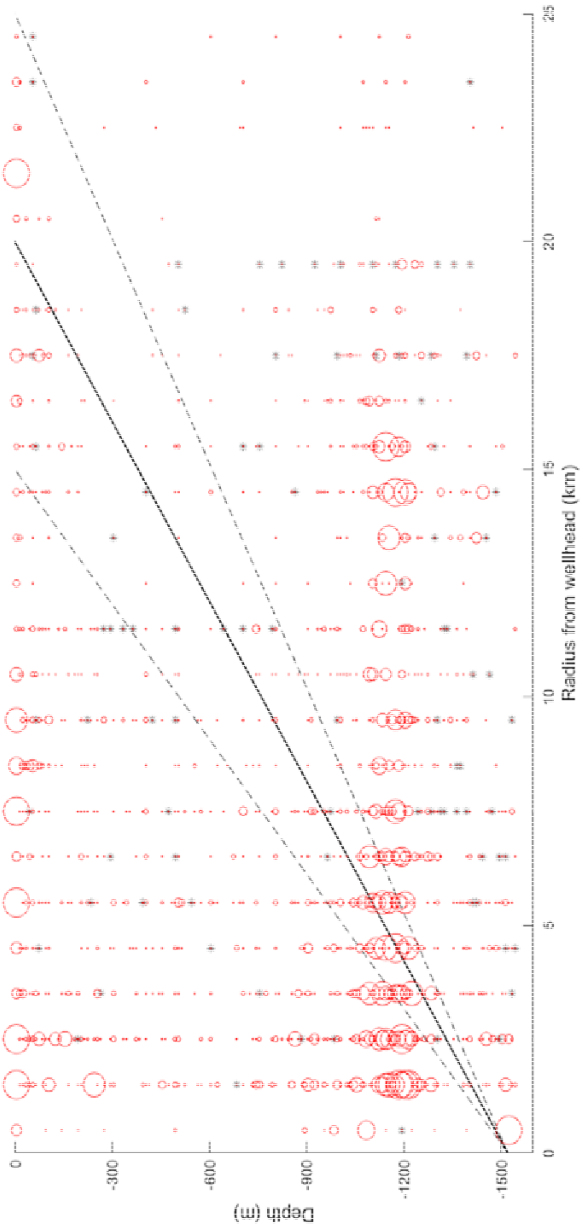

Figure 4.4. Maximum oil concentrations of all BP Gulf Science Data water samples collected from May to July, 2010. The oil concentration is computed for both hydrocarbon categories C5-C12 and C13+. Data is organized into a grid of 10 m (depth) by 1km (radial distance from wellhead) bin. The size of the red circles is proportional to the oil concentration values. Grey asterisks represent samples with zero concentration (0 µg/L). The red solid line indicates the hypotenuse of the ideal right angle, and the dashed lines represent hypotenuses with a distance from the wellhead from 15 to 25 km at the sea surface, to account for spatial variation in the tilt of the jet plume.

WORKS CITED

Aman, Zachary M., Claire B. Paris, Eric F. May, Michael L. Johns, and David Lindo-Atichati. 2015. “High-Pressure Visual Experimental Studies of Oil-in-Water Dispersion Droplet Size.” *Chemical Engineering Science* 127. Elsevier: 392–400. doi:10.1016/j.ces.2015.01.058.

Camilli, Richard, Daniela Di Iorio, Andrew Bowen, Christopher M. Reddy, Alexandra H. Techet, Dana R. Yoerger, Louis L. Whitcomb, Jeffrey S. Seewald, Sean P. Sylva, and Judith Fenwick. 2012. “Acoustic Measurement of the Deepwater Horizon Macondo Well Flow Rate.” *Proceedings of the National Academy of Sciences of the United States of America* 109 (50): 20235–39. doi:10.1073/pnas.1100385108.

Diercks, Arne R., Raymond C. Highsmith, Vernon L. Asper, Dongjoo Joung, Zhengzhen Zhou, Laodong Guo, Alan M. Shiller, et al. 2010. “Characterization of Subsurface Polycyclic Aromatic Hydrocarbons at the Deepwater Horizon Site.” *Geophysical Research Letters* 37 (20): 1–6. doi:10.1029/2010GL045046.

Fabregat Tomas, Alexandre, Andrew C. Poje, Özgökmen Tamay M., and William K. Dewar. 2016. “Effects of Rotation on Turbulent Buoyant Plumes in Stratified Environments.” *Journal of Geophysical Research: Oceans* 121 (8): 5397–5417. doi:10.1002/2016JC011737.

Graham, Bob, William K. Reilly, Frances Beinecke, Donald F. Boesch, Terry D. Garcia, and Cherry A. Murray. 2011. *Deep Water: The Gulf Oil Disaster and the Future of Offshore Drilling*. *National Commission on the BP Deepwater Horizon Oil Spill and Offshore Drilling Report to the President.* doi:10.3723/ut.30.113.

Greaves, David, John Boxall, James Mulligan, E. Dendy Sloan, and Carolyn A. Koh. 2008. “Hydrate Formation from High Water Content-Crude Oil Emulsions.” *Chemical Engineering Science* 63 (18): 4570–79. doi:10.1016/j.ces.2008.06.025.

Griffiths, Stewart K. 2012. “Oil Release from Macondo Well MC252 Following the Deepwater Horizon Accident.” *Environmental Science and Technology* 46 (10): 5616–22. doi:10.1021/es204569t.

Hénaff, Matthieu Le, Vassiliki H Kourafalou, Claire B Paris, Judith Helgers, Zachary M Aman, Patrick J Hogan, and Ashwanth Srinivasan. 2012. “Surface Evolution of the Deepwater Horizon Oil Spill Patch: Combined E Ff Ects of Circulation and Wind-Induced Drift †.”

Kessler, J D, D L Valentine, M C Redmond, M Du, E W Chan, S D Mendes, E W Quiroz, et al. 2011. “A Persistent Oxygen Anomaly Reveals the Fate of Spilled Methane in the Deep Gulf of Mexico.” *Sciencexpress* 331 (6015): 312–15. doi:10.1126/science.1199697.

Lindo-Atichati, D., C. B. Paris, M. Le Hénaff, M. Schedler, A. G. Valladares Juárez, and R. Müller. 2016. “Simulating the Effects of Droplet Size, High-Pressure Biodegradation, and Variable Flow Rate on the Subsea Evolution of Deep Plumes from the Macondo Blowout.” *Deep-Sea Research Part II: Topical Studies in Oceanography* 129. Elsevier: 301–10. doi:10.1016/j.dsr2.2014.01.011.

McNutt, Marcia, Richard Camilli, George Guthrie, Paul Hsieh, Victor Labson, Bill Lehr, Don Maclay, Art Ratzel, and Mark K. Sogge. 2011. “Assessment of Flow Rate Estimates for the Deepwater Horizon / Macondo Well Oil Spill,” 1–22.

McNutt, Marcia K, Rich Camilli, Timothy J Crone, George D Guthrie, Paul A Hsieh, Thomas B Ryerson, Omer Savas, and Frank Shaffer. 2012. “Review of Flow Rate Estimates of the Deepwater Horizon Oil Spill.” *Proceedings of the National Academy of Sciences* 109 (50): 20260–67. doi:10.1073/pnas.1112139108.

Paris, Claire B., Matthieu Le Hénaff, Zachary M. Aman, Ajit Subramaniam, Judith Helgers, Dong Ping Wang, Vassiliki H. Kourafalou, and Ashwanth Srinivasan. 2012. “Evolution of the Macondo Well Blowout: Simulating the Effects of the Circulation and Synthetic Dispersants on the Subsea Oil Transport.” *Environmental Science and Technology* 46 (24): 13293–302. doi:10.1021/es303197h.

R. Camilli, C M Reddy, D R Yoerger, B A Van Mooy, M V Jakuba, J C Kinsey, C P McIntyre, S P Sylva, and J V Maloney. 2010. “Tracking Hydrocarbon Plume Transport and Biodegradation at Deepwater Horizon.” *Sciencexpress* 330 (6001): 201–4. doi:10.1126/science.1195223.

Reddy, Christopher M, J Samuel Arey, Jeffrey S Seewald, Sean P Sylva, Karin L Lemkau, Robert K Nelson, Catherine A Carmichael, et al. 2012. “Composition and Fate of Gas and Oil Released to the Water Column during the Deepwater Horizon Oil Spill.” *Proc Natl Acad Sci USA* 109 (50): 20229–34. doi:10.1073/pnas.1101242108.

Ryerson, T. B., K. C. Aikin, W. M. Angevine, E. L. Atlas, D. R. Blake, C. A. Brock, F. C. Fehsenfeld, et al. 2011. “Atmospheric Emissions from the Deepwater Horizon Spill Constrain Air-Water Partitioning, Hydrocarbon Fate, and Leak Rate.” *Geophysical Research Letters* 38 (7): 6–11. doi:10.1029/2011GL046726.

Socolofsky, Scott A., E. Eric Adams, Michel C. Boufadel, Zachary M. Aman, ??istein Johansen, Wolfgang J. Konkel, David Lindo, et al. 2015. "Intercomparison of Oil Spill Prediction Models for Accidental Blowout Scenarios with and without Subsea Chemical Dispersant Injection." *Marine Pollution Bulletin* 96 (1–2). Elsevier Ltd: 110–26. doi:10.1016/j.marpolbul.2015.05.039.

Socolofsky, Scott A., E. Eric Adams, and Christopher R. Sherwood. 2011. "Formation Dynamics of Subsurface Hydrocarbon Intrusions Following the Deepwater Horizon Blowout." *Geophysical Research Letters* 38 (9): L09602. doi:10.1029/2011GL047174.

Spier, Chelsea, William T. Stringfellow, Terry C. Hazen, and Mark Conrad. 2013. "Distribution of Hydrocarbons Released during the 2010 MC252 Oil Spill in Deep Offshore Waters." *Environmental Pollution* 173: 224–30. doi:10.1016/j.envpol.2012.10.019.

Tolman, Richard C. 1949. "The Effect of Droplet Size on Surface Tension." *The Journal of Chemical Physics* 17 (3): 333. doi:10.1063/1.1747247.

Valentine, David L, John D Kessler, Molly C Redmond, Stephanie D Mendes, Monica B Heintz, Christopher Farwell, Lei Hu, et al. 2010. "Propane Respiration Jump-Starts Microbial Response to a Deep Oil Spill" 330 (6001): 208–11.

Wade, Terry L., Stephen T. Sweet, Jos?? L. Sericano, Norman L. Guinasso, Arne R. Diercks, Raymond C. Highsmith, Vernon L. Asper, et al. 2013. "Analyses of Water Samples From the Deepwater Horizon Oil Spill: Documentation of the Subsurface Plume." *Monitoring and Modeling the Deepwater Horizon Oil Spill: A Record Breaking Enterprise*, 77–82. doi:10.1029/2011GM001103.

Wilson, Monica, Larissa Graham, Chris Hale, Emily Maung-Douglass, Stephen Sempier, and LaDonn Swann. 2016. "Perisistence, Fate, and Effectiveness of Dispersants Used during the Deepwater Horizon Oil Spill." *Sea Grant Programs of the Gulf of Mexico*. doi:GOMSG-G-15-004.

(1) BP Gulf Science Data. 2016. Chemical analysis of oil samples from the Gulf of Mexico and adjoining states from May 2010 to March 2014

(2) Nalco Corexit 9500 Material Safety Data Sheet)

(3) BP Gulf Science Data. 2016. Subsea Dispersant Application records collected during the Deepwater Horizon (DWH) accident near the Mississippi Canyon block 252 wellhead from April 30 to July 22, 2010)

(4) BP Gulf Science Data. 2016. Surface Dispersant Application records collected during the Deepwater Horizon (DWH) accident near the Mississippi Canyon block 252 wellhead from April 22 to July 19, 2010)

(5) RStudio Team (2016). RStudio: Integrated Development for R. RStudio, Inc., Boston, MA URL http://www.rstudio.com/.

SUPPLEMENTARY INFORMATION

CHAPTER 3: SUB- SEA DISPERSANT INJECTION (SSDI) ANALYSIS

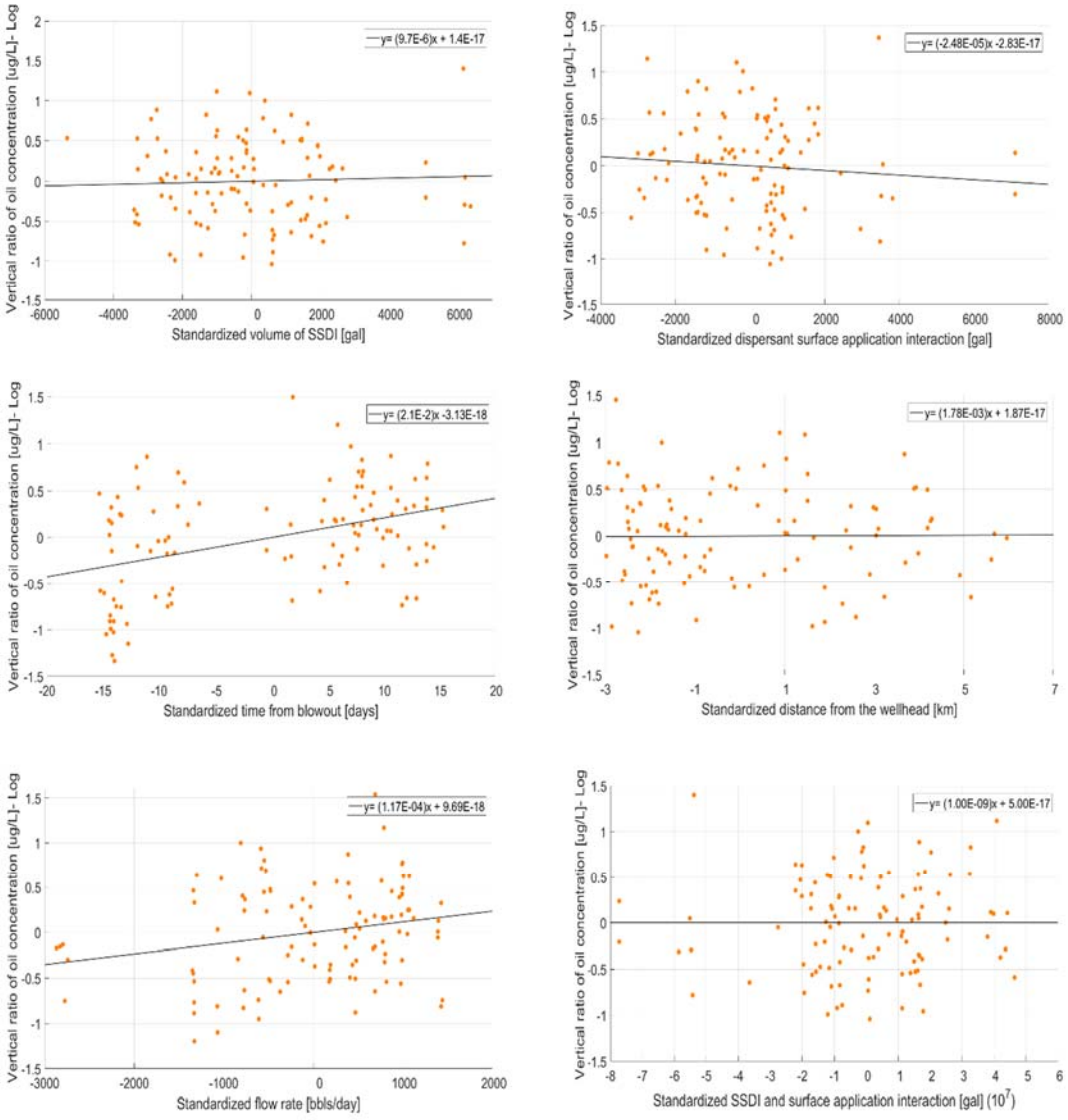

Figure S1. Robust linear regression model: 'added variable' plots of the response variable versus all the standardized explanatory variables. The data was computed within 10 km from the wellhead. Response variable: vertical concentration ratio [ug/L]: logarithmic mean oil concentration of the three upper depth ranges (i.e., 0-20 m and 20-400 m and 400-1000 m) minus the logarithmic mean oil concentration of the depth range in which the dominant intrusion layer was revealed (i.e., >=1000 m).

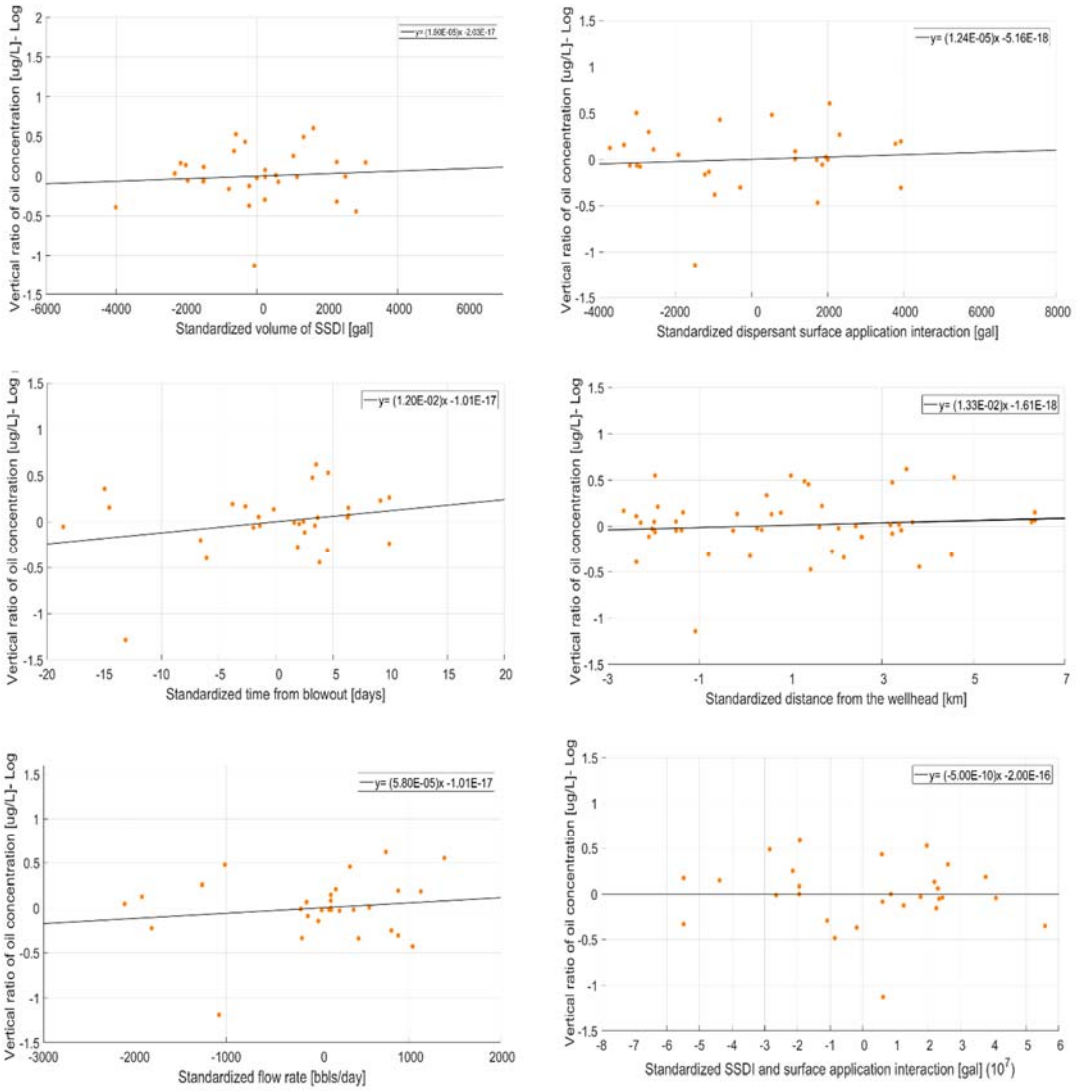

Figure S2. Robust linear regression model: 'added variable' plots of the response variable versus all the standardized explanatory variables. The data was computed within 10 km from the wellhead. Response variable: vertical concentration ratio [ug/L]: logarithmic mean oil concentration of the two upper depth ranges (i.e., 0-20 m and 20-400 m) minus the logarithmic mean oil concentration of the depth range in which the shallower intrusion layer was revealed (i.e., 400-1000 m).